Scientific Reports
https://doi.org/10.1038/s41598-025-28880-z

Article in Press

Ge/$In_{0.53}Ga_{0.47}As$ heterojunction based doping less TFET for high sensitivity label free biosensing applications

Received: 28 April 2025
Accepted: 13 November 2025
Published online: 25 November 2025

Cite this article as: Jaya M. & Lorenzo R. Ge/$In_{0.53}Ga_{0.47}As$ heterojunction based doping less TFET for high sensitivity label free biosensing applications. *Sci Rep* (2025). https://doi.org/10.1038/s41598-025-28880-z

Mandalaneni Jaya & Rohit Lorenzo

Ge/$In_{0.53}Ga_{0.47}As$ Heterojunction Based Doping Less TFET for High Sensitivity Label Free Biosensing Applications

Mandalaneni Jaya[1], Rohit Lorenzo*[2]
[1,2]School of Electronics Engineering, VIT-AP University, Amaravati, India, 522237.
Email: jaya.22phd7011@vitap.ac.in[1],rohit.lorenzo@vitap.ac.in*[2]
Corresponding Author Email: rohit.lorenzo@vitap.ac.in

Abstract:

In this paper, a drain-engineered Ge/$In_{0.53}Ga_{0.47}As$ heterojunction-based doping less TFET (DE-HJ-DLTFET) is proposed for label-free biosensing applications. To reduce the fabrication cost and random-dopant-fluctuation (RDF) effects, a doping-less TFET is considered a biosensor. A Ge/$In_{0.53}Ga_{0.47}As$ heterojunction is regarded at the source-channel interface to reduce the potential barrier, thus improving the DE-HJ-DLTFET drain current (I_{DS}) and SS value. Then, a small metal strip is inserted in the oxide region above the source-channel interface to improve the BTBT rate and I_{DS} for the proposed device at low gate voltages. Moreover, a drain metal with a combination of two different work function metals is considered to reduce leakage current (I_{OFF}) and ambipolar conduction in the DE-HJ-DLTFET. As a result, the proposed DE-HJ-DLTFET shows remarkable I_{DS} sensitivity and turn-on voltage sensitivity of ~10^8, 0.85 in comparison to other advanced biosensors. Performance is evaluated under the influence of varying biomolecular charges. Furthermore, the improvement in ON-current and reduced I_{OFF} improved the I_{ON}/I_{OFF} sensitivity of the DE-HJ-DLTFET biosensor under the presence of different biomolecular charges. Therefore, these improvements in I_{DS}, turn-on, and I_{ON}/I_{OFF} sensitivity make the DE-HJ-DLTFET a good candidate for next-generation low-power sensing applications.

***Keywords*—Dielectric modulation, Sensitivity, Biosensor, Nano-cavity.**

I. INTRODUCTION

The main goal of medical healthcare devices is to accurately measure health status, detect disease onset, and track progression [1]. Consequently, there is a critical need for user-friendly biosensors, easy to dispose of compassionate, fast in response, suitable for mass production, and cost-effective for medical diagnostics. The development of highly responsive handheld biosensors with improved durability, robustness, and efficiency is an urgent need for the current generation. The label-free detection approach using field-effect transistors (FETs) ensures high accuracy while preserving the intrinsic characteristics of biomolecules. [2]. Although FET-based devices are compact and cost-effective, they encounter significant scaling issues, including short-channel effects (SCEs), increased off-state leakage, and a higher subthreshold swing(SS) leads to more power consumption in MOSFETs [3]-[4]. In addition, FET-based biosensors face significant challenges, including low sensitivity and long response times for the detection of biomolecules due to physical limitations at room temperature. Several other critical issues such as random doping fluctuations, fabrication complexities, and high costs associated with annealing processes [5]-[7].

To overcome these challenges, various tunnel-FET-based biosensors have been proposed, offering properties such as steep SS, low power consumption, fast response times, and high sensitivity [8-11]. However, physically doped TFETs face challenges such as statistical stochastic dopant variations and fabrication complexity in achieving sharp doping profiles at the channel-drain (C-D) and source-channel (S-C) junctions [12]. To address these challenges, doping less-TFET-based devices have been introduced, offering several advantages including reduced fabrication complexity, lower thermal budget, and improved scalability [13]-[18].

However, the dopingless TFET-based biosensor is limited by low sensitivity because it exhibits a lower tunneling rate S-C interface in the presence of different biomolecules [19-21].

Therefore, this manuscript introduces a novel drain-engineered heterojunction dopingless TFET (DE-HJ-DLTFET) to address the abovementioned issues. In this structure, the Ge-In0.53Ga0.47As-based hetero junction decreases the width of the barrier at the (C-S) interface. Thereafter, a small metal strip is inserted in the oxide between the C-S interface helping to enhance the tunneling rate thereby SS value for the proposed device. Hence, this improvement in SS value improves the responsiveness of the DE-HJ-DLTFET to various biomolecules.In addition, the drain metal is a combination of two different work function materials, which induces a high bandgap at the C-D interface. This further helps to prevent leakage current and ambipolar conduction in the DE-HJ-DLTFET. Therefore, the minimization of off-state current leakage (I_{OFF}) in the proposed device helps to improve the I_{ON}/I_{OFF} ratio thereby I_{ON} to I_{OFF} ratio (CSR) sensitivity of the DE-HJ-DLTFET. The inclusion of a thin SiO_2 layer beneath the cavity not only prevents native oxide formation but also acts as an adhesive for biomolecules, enhancing the reliability of biosensing applications.

II. DEVICE ARCHITECTURE AND SIMULATION TECHNIQUES

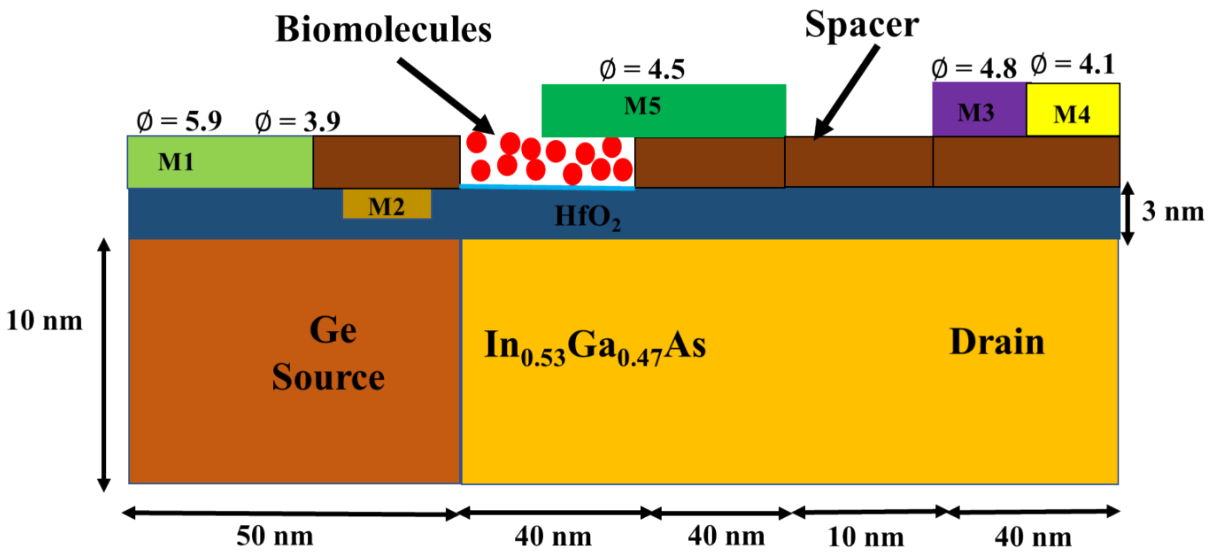

(a)

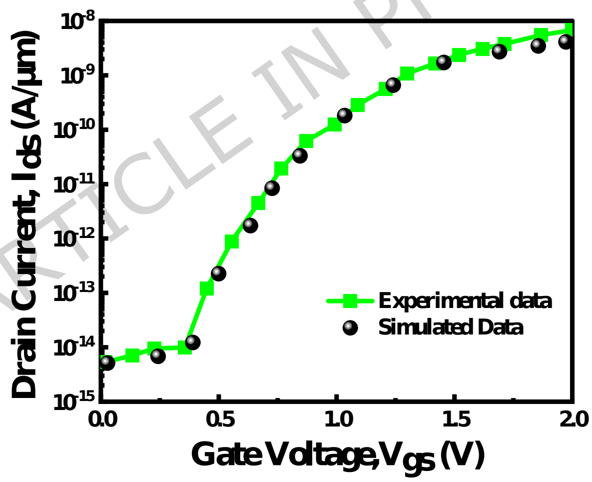

(b)

ARTICLE IN PRESS

Fig. 1(a). 2D diagram of the proposed DE-HJ-DLTFET biosensor. **(b)** Calibration of the simulation results of the proposed device with experimental results [24].

The 2D schematic of the drain-engineered heterojunction doping-less TFET (DE-HJ-DLTFET)-based biosensor is illustrated in Fig.1(a). This design incorporates a Ge/In0.53Ga0.47As heterojunction to enhance band-to-band tunneling (B2BT) at the C-S interface [22]. Metal electrodes with suitable work functions are used to form the source and drain regions. The lengths of the source, gate, and drain metals are set at 50 nm, 40 nm, and

40 nm, respectively. To mitigate short-channel effects and improve subthreshold behavior, spacers are added at the interfaces between the source, gate, and drain metals. A 5 nm thick cavity layer is positioned near the source side to influence the device's electrical characteristics. To prevent gate-to-channel leakage current and protect the cavity from native oxide formation due to air exposure, a 1 nm thick SiO_2 layer is placed beneath the cavity. A 3 nm long metal strip is added to the oxide region at the S-C interface. Additionally, to minimize ambipolar conduction and leakage currents, two metal layers (M3 and M4) with work functions of 4.8 eV and 4.1 eV are placed over the drain region, and the thickness is 5 nm.

All the simulations of the proposed DE-HJ-DLTFET are carried out using the Sentaurus TCAD tool. [23]. For that, advanced physical models are incorporated to evaluate the device parameters accurately. A nonlocal Band-to-Band Tunneling (BTBT) model is employed to examine the tunneling probability at the source-channel interface. To evaluate carrier recombination and generation in the device, both the Shockley–Reid–Hall (SRH) and Auger recombination models are employed. The electric field-dependent mobility (FLDMOB) model is incorporated to account for the impact of high electric fields on carrier mobility [24]. While trap-assisted tunneling (TAT) mediated by interface traps is known to significantly increase leakage current and limit subthreshold swing in TFETs [25], the present study deliberately omits the TAT model to focus on intrinsic band-to-band tunneling. Therefore, the reported performance represents an idealized upper limit. To ensure physical accuracy, the BTBT model used in this work was adapted following the experimental calibration methodology reported by Smets et al. [24]. Although their calibration was based on a GaAsSb/InGaAs heterojunction, we did not use GaAsSb material parameters in our simulations. Instead, all material-dependent properties such as the bandgap (E_g), electron affinity (χ), and effective tunneling mass (m) were substituted with experimentally reported values specific to the Ge/$In_{0.53}Ga_{0.47}As$ interface. The Smets calibration was employed only as a methodological framework to validate the BTBT formulation and ensure convergence accuracy. This adaptation enables reliable prediction of intrinsic tunneling behavior while maintaining physical consistency with the proposed device. It is acknowledged that direct experimental calibration using fabricated Ge-source TFET prototypes will be pursued in future work to further refine interface-specific effects. Additionally, Fermi-Dirac statistics and KLA models are utilized to capture the effects of lateral electric fields on carrier mobility, providing a reliable representation of charge transport under different bias conditions. Thereafter, the drift-diffusion transport model is applied to simulate carrier flow and current characteristics with high accuracy, ensuring a comprehensive understanding of the device's performance. The effective masses of electrons and holes are considered as 0.22m0 and 0.51m0, respectively, where m0 is the rest mass of an electron. The device simulations also incorporate quantum effects due to the thin body thickness (T_{body}=10 nm), which is less than the Debye length, suppressing short-channel effects. The proposed DE-HJ-DLTFET structure is further calibrated with experimental data from prior work to validate [24]. The simulation results we found that results closely matched the experimental data, as depicted in Fig. 1(b). These calibration steps ensure standardization and consistency in the models and methodologies employed.

III. RESULTS AND DISCUSSION

This section presents the I_D-V_{GS} characteristics of the drain-engineered heterojunction doping-less TFET (DE-HJ-DLTFET) are analyzed by varying the dielectric constants (K) of trapped biomolecules within the cavity. The dielectric constant (K) values for the biomolecules are considered as K = 1, 2, 5, 7, and 10, corresponding to different biomolecular environments. The dielectric constants used in the study represent common biomolecules such as DNA (K2-4), proteins (K4-6), and enzymes or antibodies (K~7-10). Additionally, the analysis includes the effect of neutral, positive, and negative charge biomolecules on the device's performance. The effect of varying probe placements is also investigated to assess its influence on the sensitivity and overall characteristics of the DE-HJ-DLTFET. This comprehensive evaluation provides insights into the role of biomolecular charges and probe positioning in optimizing the device for sensing applications. To observe the I_D-V_{GS} characteristics of the DE-HJ-DLTFET, the charge of the biomolecules is taken as neutral, and the drain-to-source voltage (V_{DS}) is fixed at 1 V, as shown in Fig. 2(a).

3.1 Neutral Biomolecules: Impact on DE-HJ-DLTFET Performance with Varying Dielectric Constants

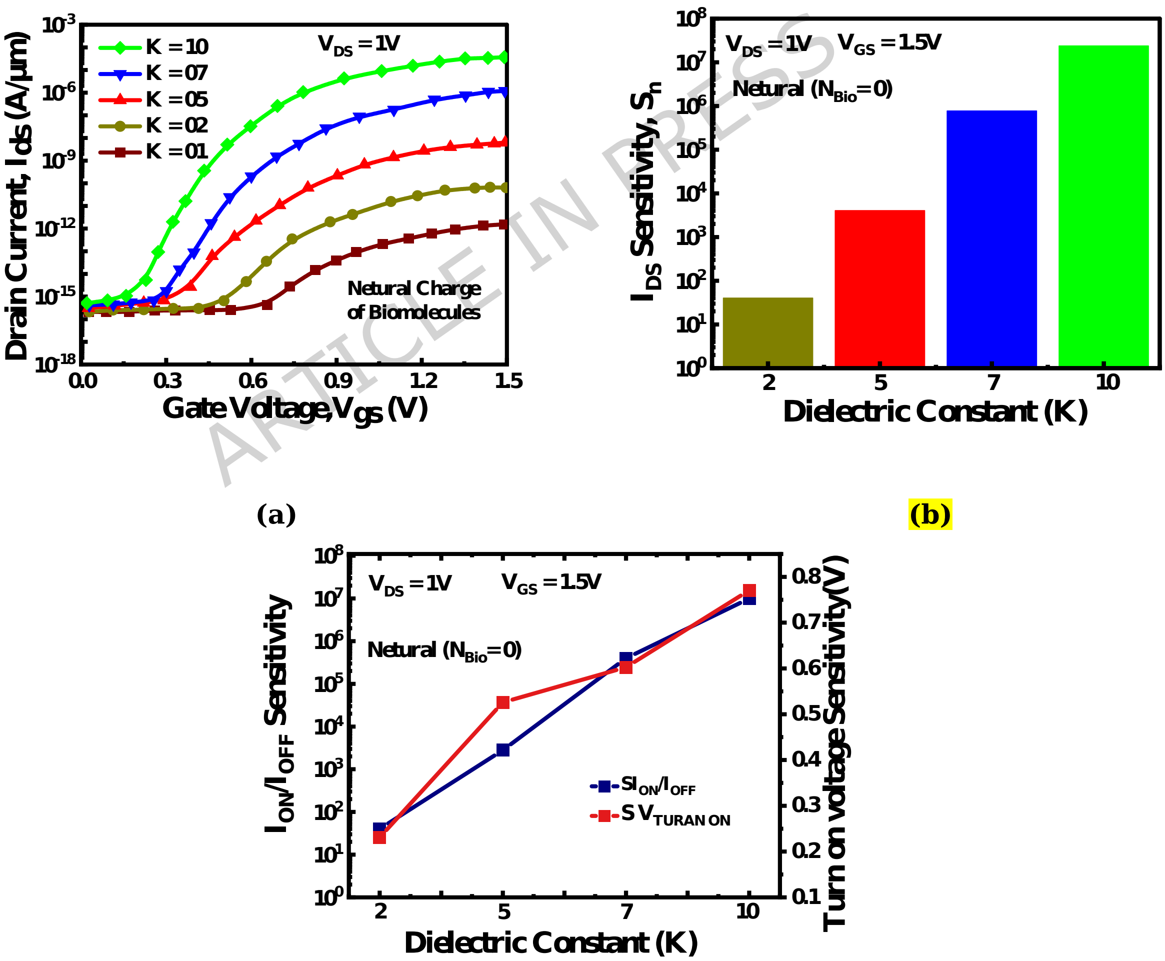

(c)

Fig. 2. (a) I_D-V_{GS} characteristics, **(b)** I_{DS} sensitivity, **(c)** I_{ON}/I_{OFF}, and turn-on voltage sensitivity of the DE-HJ-DLTFET by varying the K values.

Fig. 2(a) demonstrates a clear dependence of drain current (I_{DS}) on the gate voltage (V_{GS}) and the dielectric constant of the biomolecules for the proposed DE-HJ-TFET. At K=1, the dielectric constant of biomolecules becomes low, and the tunneling current remains relatively small throughout the voltage sweep due to weak electrostatic modulation across the tunneling junction. As the dielectric constant increases, the I_{DS} curve shifts upward due to an enhancement in the tunneling current. This behavior can be attributed to the enhanced electric field coupling at the source-channel interface with increasing K. The I_{ON} is found to be high at K=10 which is mainly because the higher dielectric constant amplifies the potential drop across the tunneling junction, and enhances the band-to-band tunneling probability at the S-C interface. Since the proposed device consists of Ge/$In_{0.53}Ga_{0.47}As$ based heterojunction and lowers the bandgap across the S-C interface. Moreover, the insertion of a small metal strip above the S-C interface helps in enhancing the carrier tunneling rate at lower gate voltages. As a result of this, I_{ON} and SS value is found to be improved while increasing the K values for the proposed device. It is well known that, the drain current sensitivity also depends on the SS value of the DE-HJ-DLTFET biosensor. It can be evident from Fig. 2(b) that, I_{DS} sensitivity is found to be increased when the K of the biomolecules increases from K=2 to 10. This trend reflects the enhancement of the device response concerning the variations in the K of the biomolecules within the cavity region. TheI_{DS} sensitivity value is found to be a maximum of ~10^8orders at K=10. Therefore, this significant improvement in I_{DS} sensitivity value makes the DE-HJ-DLTFET a promising contender for biosensing applications.

Furthermore, the implementation of metal-drain engineering (DE) in the DE-HJ-DLTFET exhibits excellent suppression of ambipolar conduction and reduces the leakage currents (I_{OFF}) in the subthreshold region. This further helps to achieve high CSR sensitivity in the DE-HJ-DLTFET which is very crucial for the biosensing applications. Fig. 2(c) illustrates the CSR sensitivity of the DE-HJ-DLTFET by varying dielectric constants (K) of neutral biomolecules at a V_{GS} of 1.5 V. At K=2, the DE-HJ-DLTFET shows an insignificant increase in the CSR sensitivity, which is in the order of ~10^2. It is mainly because the biomolecules with a less Kinducea very small I_{ON} value, which eventually reduces the I_{ON}/I_{OFF} sensitivity of the proposed device. As the K value rises to 5, a noteworthy increase in the CSR sensitivity is observed, which is mainly due to the enhanced electrostatic coupling across the device's tunneling junction. This enhanced coupling leads to reduce the bandgap and increases the tunneling current at lower V_{GS}. Furthermore, at K=10, the CSR sensitivity is found to be a maximum of ~10^7. This improvement in CSR sensitivity helps to reduce the noise involvement in the proposed biosensor. This is critical for detecting small variations in the concentration of biomolecules in biosensing environments. Thereafter, at K=10, the tunneling current is significantly modulated by the biomolecules, resulting in a sharp increase in current at a relatively low gate voltage. Since, the higher dielectric constant materials enhance the electric field coupling at the C-S interface, which, in turn, increases the probability of band-to-band tunneling at lower gate voltages. Fig. 2(c) also illustrates the turn-on voltage variation of the proposed DE-HJ-DLTFET with increasing dielectric constant (K=2,5,7,10) in the neutral biomolecular charge state. It can be evident from Fig. 2(c) that, the DE-HJ-DLTFETs show better turn-on voltage sensitivity at K=10. The turn-on voltage also increases with K, reflecting enhanced gate-to-channel coupling and increased tunneling barrier width. This behavior highlights the device's suitability for detecting biomolecules with varying dielectric properties. The observed trends validate the DE-HJ-DLTFET's robust performance for biosensing applications.

Drain current sensitivities (S_{Id})

$$\frac{I_{d\varepsilon k>1}(bio) - I_{d\varepsilon k=1}(air)}{I_{d\varepsilon k=1}(air)} \quad \textbf{(1)}$$

I_{ON}/I_{OFF} (CSR) ratio sensitivities SI_{ON}/I_{OFF}

$$\frac{I_{ON}}{I_{OFF}} = \frac{\frac{I_{ON}}{I_{OFF}}\Big|_{\varepsilon k>1} - \frac{I_{ON}}{I_{OFF}}\Big|_{\varepsilon k=1}}{\frac{I_{ON}}{I_{OFF}}\Big|_{\varepsilon k=1}} \quad \textbf{(2)}$$

Turn- ON voltage sensitivities

$$V_{Turn\text{-}ON} = V_{Turn\text{-}ON\varepsilon k>1}(bio) - V_{Turn\text{-}ON\varepsilon k=1}(air) \quad \textbf{(3)}$$

Negative Charge Biomolecules on Sensitivity

$$V_{gs} = \varnothing_s + \varnothing_{ms} + \left\{\frac{-q(\pm N_{bio})}{\Delta_c}\right\} \quad \textbf{(4)}$$

The sensitivity analysis of the proposed DE-HJ-DLTFET is evaluated using key metrics derived from the given equations. The drain current sensitivity (SI_d) [Equation (1)] [26] quantifies the variation in current due to biomolecule immobilization, comparing dielectric constants (εk> 1) with air (εk = 1). The CSR current ratio sensitivity[Equation (2)] [27] highlights the change in device switching characteristics caused by biomolecular environments. Turn-ON voltage sensitivity [Equation (3)] [28] assesses shifts in $V_{Turn\text{-}ON}$ due to biomolecule-induced changes. For negatively charged biomolecules, gate-to-source voltage depends on biomolecular charge density, as shown in Equation (4) [29]. This affects device sensitivity and enables precise characterization of biomolecule interactions in the nano-cavity.

3.2 Positive charge Biomolecules: Influence on $I_D\mathbf{-}V_{GS}$ Characteristics of DE-HJ-DLTFET

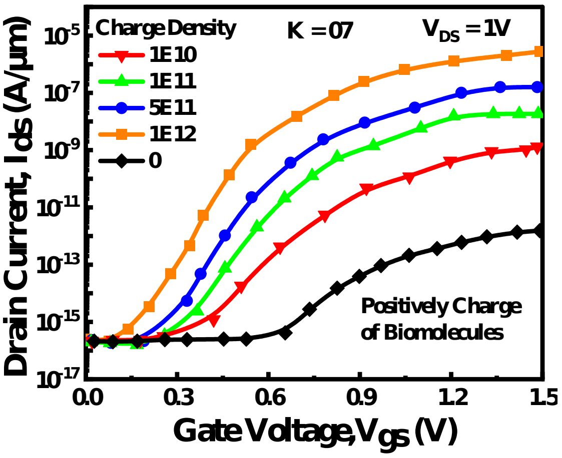

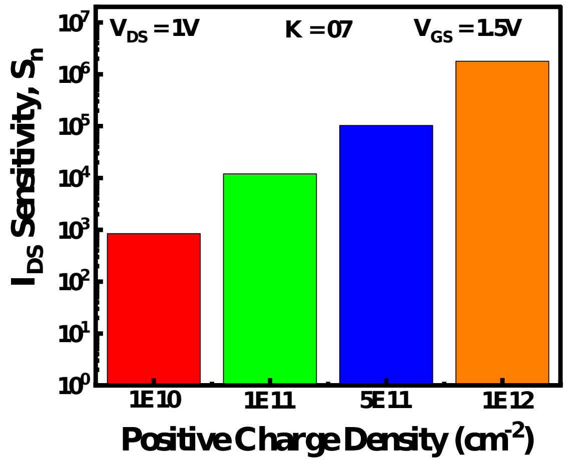

(a)

(b)

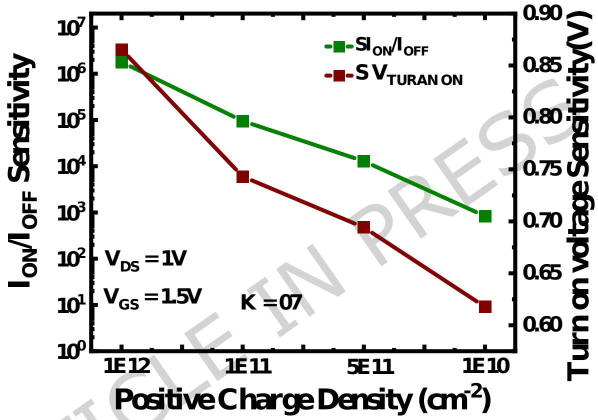

(c)

Fig. 3. (a) $I_D - V_{GS}$ characteristics **(b)** I_{DS} sensitivity, **(c)** $I_{ON}/I_{OFF,}$ and turn-on voltage sensitivity of the proposed DE-HJ-DLTFET by varying the positive charge densities.

To verify the performance parameters like $I_{DS,}$ $I_{ON}/I_{OFF,}$ and turn-on voltage sensitivity of the DE-HJ-DLTFET in the presence of positively electrostatic charged biomolecules, the dielectric constant of the biomolecules is fixed at K=7. Fig.3(a) demonstrates the $I_D - V_G$ transfer characteristics of the proposed DE-HJ-DLTFET-based biosensor by varying the positive charge from 1E10 to 1E12. As the positive charge density increases from 1E10 to 1E12, the drain current (I_{DS}) rises significantly and is reported to be high at 1E12. This increment in I_{DS} is mainly due to the incidence of a positive electrostatic charge in the cavity improves the electrostatic coupling at the source-channel interface. As a result of this, the tunneling-barrier-width becomes reduced and the BTBT rate gets improved at the C-S interface. Fig. 3(b) depicts the I_{DS} sensitivity variation by increasing positive biomolecular charge in the proposed device. The I_{DS} sensitivity found to be high at 1E12. Fig. 3(c) shows the enhancement in I_{ON}/I_{OFF} sensitivity, and turn-on voltage sensitivity while increasing the positive charge densities. The I_{ON}/I_{OFF} sensitivity improvement in the DE-HJ-DLTFET is primarily due to the significant improvement in I_{ON} without degrading the I_{OFF}. Moreover, the turn-on voltage sensitivity also improved for the DE-HJ-DLTFET in the presence of positive electrostatic charges. It is mainly because of the presence of positive charges that the effective tunneling barrier width gets reduced and the BTBT rate into the channel becomes high at lower gate voltages.

3.3 Negative charge Biomolecules: Influence on $I_D - V_{GS}$ Characteristics of DE-HJ-DLTFET

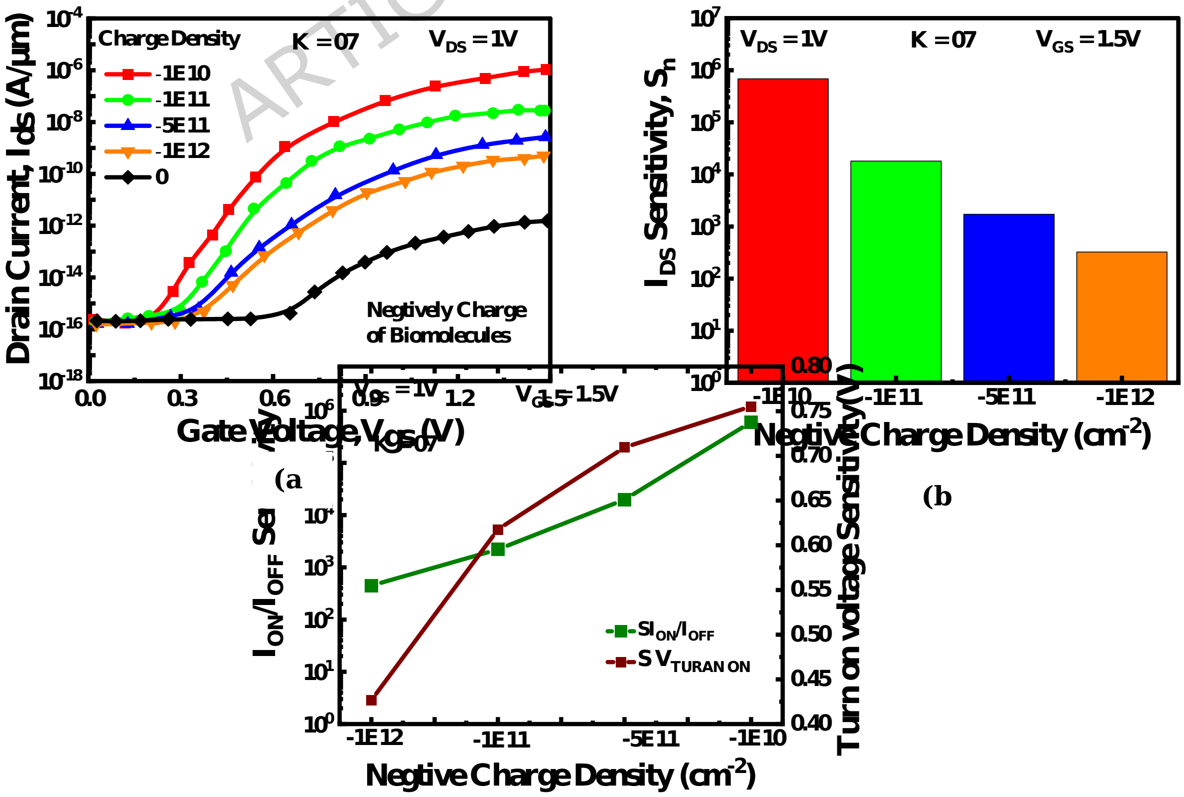

(c

Fig. 4. (a)$I_D{-}V_{GS}$ characteristics, **(b)** I_{DS} sensitivity, **(c)** $I_{ON}/I_{OFF,}$ and turn-on voltage sensitivity of the proposed DE-HJ-DLTFET by varying the negative charge densities.

Fig. 4(a) illustrates the $I_D{-}V_G$transfer characteristics of the DE-HJ-DLTFET in the incidence of negatively electrostatic charged biomolecules when the dielectric constant of the biomolecular charge is fixed at (K=7). As the negative electrostatic charge density increases from -1E10 to -1E12, the drain current (I_{DS}) is found to decrease in the proposed DE-HJ-DLTFET. The I_{DS} is reported to be high of ~10^{-6} A/µmat -1E10 charge density. When it comes to -1E12, the I_{DS} is degraded to ~10^{-11} A/µm. It is mainly due to the reduction of electrostatic coupling at the C-S interface enhances the width of the tunneling barrier and reduces the carrier tunneling rate into the channel region. The I_{DS} sensitivity of the DE-HJ-DLTFET is reduced when the increment of the negative biomolecular charge is as depicted in Fig. 4(b). As the increase of negative charge density in the cavity area reduces the gate electric field at the C-S interface, it leads to a small increase of I_{ON} in the DE-HJ-DLTFET at lower V_{GS}.

Fig. 4(c) illustrates the reduction of current-switching-ratio (CSR) sensitivity, and turn-on voltage sensitivity at higher negative charge densities. The CSR ratio decreases due to the degradation of the I_{ON}, while I_{OFF} remains constant. Moreover, the turn-on voltage sensitivity is also reported to be degraded with the increment of the negative

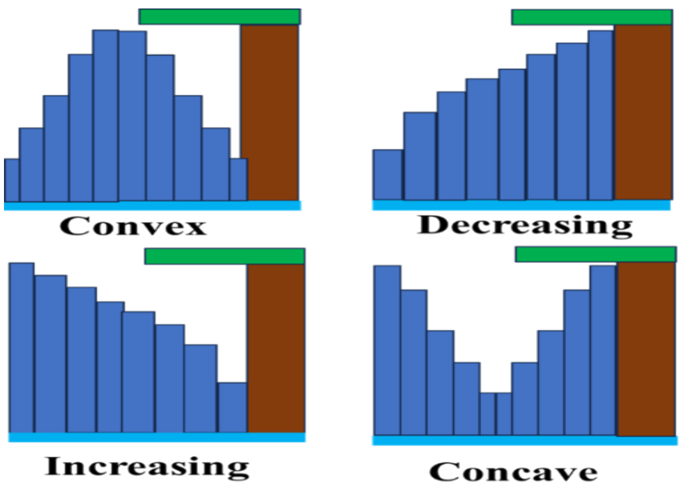

charge densities in the proposed device. Since, the negative charges widen the effective tunneling barrier, making the device less responsive to charge variations at lower V_{GS}. Therefore, it is necessary to limit the concentration of negatively charged biomolecules to a lower order to attain high sensitivity for the DE-HJ-DLTFET biosensor. Hence, the obtained outcomes reveal that the DE-HJ-DLTFET-based biosensor can detect the biomolecules effectively in the presence of different biomolecular charge densities.

Fig. 5. Different types of biomolecule circulation in the cavity region of the proposed DE-HJ-DLTFET.

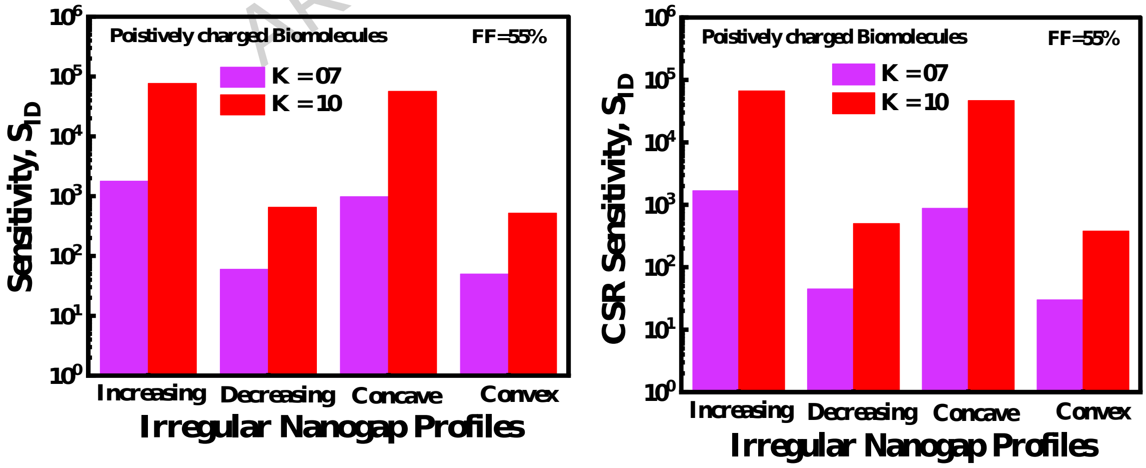

(a

(b

Fig. 6. (a) Drain current sensitivity and **(b)** CSR sensitivity of the proposed DE-HJ-DLTFET when positively charged biomolecules are distributed in irregular nanogap profiles.

Fig. 5 represents the possible biomolecular distributions, like concave, convex, decreasing, and increasing profiles in the nanocavity region of the proposed DE-HJ-DLTFET. To analyze the I_D and CSR sensitivity of the proposed device, positively charged biomolecules with dielectric constants of K=7 and K=10 are considered in the form of irregular nanogap profiles as shown in Fig. 6(a)-(b). It can be observed from Fig. 6(a) that, the I_D sensitivity is found to be high in the case of K=10 as compared to K=7 in the proposed biosensor. This is mainly owing to the presence of high-K positive electrostatic charged biomolecules, increasing the gate-to-channel coupling and carrier BTBT rate at the C-S interface. Thereafter, the CSR sensitivity is also found to be high for the proposed biosensor while considering the high-k biomolecules at irregular nanogap profiles. Since the high-k positive creates a stronger electrostatic field at the C-S interface. This effect lowers the tunneling barrier, significantly enhancing the on-state current (I_{ON}) while maintaining a low I_{OFF}.In contrast, convex and decreasing profiles exhibit relatively lower I_D and CSR sensitivity when compared to concave and increasing profiles in the cavity region. This is mainly due to the proposed device cavity with convex and decreasing profiles induces weaker charge modulation and less effective coupling at the interface. These results emphasize the importance of both dielectric constant selection and biomolecular distribution in optimizing I_D and CSR sensitivity in the case of anomalous biomolecular profiles. The findings confirm the suitability of the DE-HJ-DLTFET for detecting complex biomolecular arrangements, with concave and rising profiles providing optimal performance at high K.

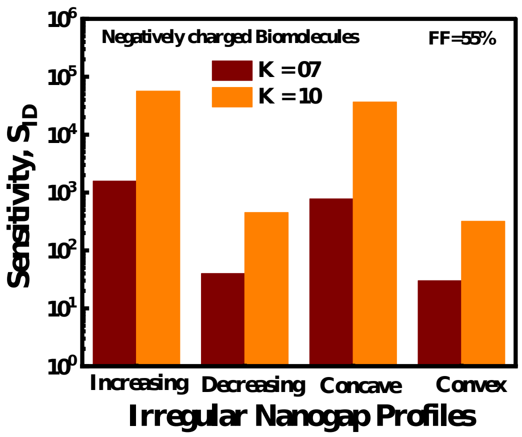

(a)

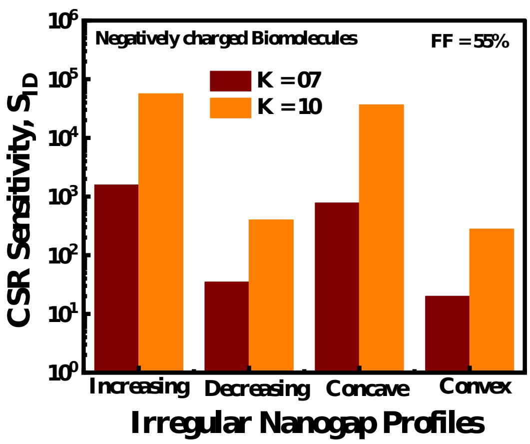

(b)

Fig. 7. (a) I_D sensitivity and (b) CSR sensitivity of the DE-HJ-DLTFET when negatively charged biomolecules are distributed in irregular nanogap profiles.

Fig. 7(a) depicts the I_D sensitivity of the DE-HJ-DLTFET in the presence of irregularly distributed negatively charged biomolecules (concave, convex, decreasing, and increasing profiles). To do so, the K of the biomolecules is considered as K=7 and K=10, respectively. The negatively charged biomolecules influence the device characteristics by inducing an opposite potential near the C-S interface, which alters the tunneling barrier and carrier transport. The results show that higher I_D and CSR sensitivities are observed at K=10compared to K=7 in the case of irregularly distributed negatively charged biomolecules in the proposed device, as shown in Fig. 7(b). However, the negative charge reduces the tunneling barrier more significantly, resulting in an increase in the ON-current and a sharper response in sensitivity. Among the profiles, concave and increasing distributions of negatively charged biomolecules exhibit the highest sensitivity and CSR ratios, as they concentrate more charge near the tunneling junction, thereby enhancing band-to-band tunneling (BTBT) probability. These profiles maximize the interaction between the negative biomolecular potential and the device's electrostatics, particularly at higher K values. In comparison, convex and decreasing profiles show relatively lower sensitivity and CSR ratios, due to weaker modulation effects at the tunneling junction. Nonetheless, the higher dielectric constant at K=10 compensates for this limitation, resulting in improved device performance compared to K=7. The 55% fill factor ensures adequate interaction of the negatively charged biomolecules with the device cavity, balancing sensitivity, and operational stability. These results validate the DE-HJ-DLTFET's capability to detect negatively charged biomolecules effectively and emphasize the critical role of biomolecular charge type, distribution, and dielectric constant in optimizing biosensor performance. The DE-HJ-DLTFET demonstrates a strong dependence on the occurrence of biomolecules and the K of the surrounding medium, making it an excellent candidate for biosensing applications. Furthermore, the device's sensitivity improves significantly with an increase in the fill factor, corresponding to the active area occupied by biomolecules, as

Case	The shaded area represents the presence of biomolecules	Fill Factor	Sensitivity		
			K=5	K=7	K=10
1	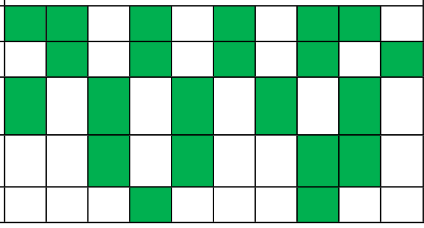	80%	2.9×10^4	1.1×10^5	2.7×10^6
2		70%	3.1×10^3	2.2×10^4	1.4×10^5
3		60%	1.5×10^2	4.1×10^3	4.5×10^4
4		50%	3.4×10^1	3.6×10^2	4.8×10^3
5		40%	2.1×10^1	2.5×10^1	2.3×10^2

shown in Table 1. A higher number of biomolecules enhances the device's electric field modulation, reducing the tunneling barrier and enabling stronger current flow, which translates to improved sensitivity. Conversely, when the fill factor decreases, the sensitivity drops, highlighting the critical role of biomolecule coverage in determining the device's performance.

3.4 Effect of Symmetric Biomolecule Interaction and Probe Placement in Nano-Cavity Sensors

Table 1: Probe placement of the DE-HJ-DLTFET biosensor for the different biomolecules.

Additionally, the K of the environment adjacent the biomolecules have a profound impact on sensitivity. As the K enhances, the gate-to-channel coupling improves, which enhances the tunneling current and results in a substantial increase in sensitivity. This exponential improvement suggests that incorporating high-K materials or optimizing the dielectric environment can significantly boost the device's detection capabilities. In contrast, at lower dielectric constants, the sensitivity remains limited, even for higher biomolecular presence. The DE-HJ-DLTFET biosensor achieves superior performance when the biomolecular coverage is maximized, and the K of the medium is high. These observations emphasize the importance of material engineering, surface fictionalization, and optimization of the sensing environment to achieve highly sensitive and efficient biosensors. The device's capability to demonstrate exponential sensitivity enhancement under optimized conditions makes it a highly promising platform for innovative biosensing applications.

3.5 Benchmarking

The proposed DE-HJ-DLTFET-based biosensor shows remarkable improvement in drain current sensitivity when compared to other advanced biosensors, as shown in Table 2. It is mainly because the substantial improvement of I_{ON} and SS values in the DE-HJ-DLTFET increases the drain sensitivity as conventional biosensors like Dielectric-Modulated FET (DM-FET), Negative Capacitance TFET (NC-TFET), and MOSFET-Based Biosensor. However, the Double-Gate TFET and Split-Gate TFET-Based Biosensors show moderate improvements but still do not surpass the sensitivity of DE-HJ-DLTFET. Few other biosensing devices, such as L-shaped gate TFET (LTG-TFET) and source-drain engineered TFET (SDE-TFET), perform better than conventional sensors, although still lower than the best sensitivity of DE-HJ-DLTFET. Therefore, the improved sensitivity in DE-HJ-DLTFET makes it a highly effective candidate for next-generation biosensing applications.

Device	**I_{DS} Sensitivity**
Dielectric-Modulated FET (DM-FET) [30]	1×10^4
Negative Capacitance TFET (NC-TFET) [31]	5×10^5
MOSFET-Based Biosensor [32]	1×10^3
Double-Gate TFET Biosensor [33]	7×10^5
Split-Gate NCTFET-Based Biosensor [34]	2×10^6
L-Shaped Gate TFET (LTG-TFET) [35]	4×10^6
Source-Drain Engineered TFET (SDE-TFET) [36]	5×10^6
T-shaped silicon channel [37]	6.95×10^5

Proposed Device	5×10^{7}

Table 2: I_D sensitivity assessment of the DE-HJ-DLTFET-based biosensor with other state-of-the-art TFET based biosensors.

IV. CONCLUSION

This manuscript presents a drain-engineered Ge/In0.53Ga0.47As heterojunction doping less TFET (DE-HJ-DLTFET) based biosensor to detect the various biomolecules effectively. Simulation results reveal a significant improvement in drain current sensitivity, CSR sensitivity, and turn-on voltage sensitivity obtained for the DE-HJ-DLTFET in the presence of different biomolecular charges. This improvement in I_D sensitivity and turn-on voltage sensitivity is mainly due to the presence of Ge/In0.53Ga0.47A heterojunction, which reduces the potential barrier. It increases the drain current at the S-C interface at low gate voltages. Then, the drain metal engineering method helps to reduce the leakage current, thereby increasing the CSR sensitivity in the proposed biosensor. Furthermore, biomolecules with high-k value showed better sensitivity in the proposed biosensor at the maximum fill factor in the cavity region.

Data availability

The datasets generated and/or analysed during the current study are not publicly available due to the proprietary nature of the simulation environment and large file sizes, but are available from the corresponding author on reasonable request.

Conflict of Interest

The authors declare no competing interests.

Acknowledgement

Authors are thankful to VIT-AP University for providing computational resources.

Authors Contribution

M Jaya: Design and analysis, writing original draft; **R Lorenzo:** Review, editing, and supervision.

V. REFERENCES

1. Young KK. Short-channel effect in fully depleted SOI MOSFETs. IEEE Trans Electron Devices 1989; 36: 399-402.
2. Narayanan M, Al-Nashash H, Mazhari B, Pal D Chandra M. Analysis of kink reduction in SOI MOSFET using selective back oxide structure. Active Passive Electron. Compon. 2012; Article ID 565827, 1-9
3. Kumari, M., Singh, N. K., Sahoo, M., & Rahaman, H. (2021). Work function optimization for enhancement of sensitivity of dual-material (DM), double-gate (DG), junctionless MOSFET-based biosensor. *Applied Physics A*, *127*, 1-8.
4. Narang, R., Saxena, M., & Gupta, M. (2015). Comparative analysis of dielectric-modulated FET and TFET-based biosensor. *IEEE Transactions on Nanotechnology*, *14*(3), 427-435.
5. Hafiz, S. A., Ehteshamuddin, M., & Loan, S. A. (2019). Dielectrically modulated source-engineered charge-plasma-based Schottky-FET as a label-free biosensor. IEEE Transactions on Electron Devices, 66(4), 1905-1910.
6. Rashid, S., Bashir, F., Khanday, F. A., & Beigh, M. R. (2022). Dielectrically modulated III-V compound semiconductor based pocket doped tunnel FET for label free biosensing applications. *IEEE Transactions on NanoBioscience*, *22*(1), 192-198.
7. Kanungo, S., Chattopadhyay, S., Gupta, P. S., Sinha, K., & Rahaman, H. (2016). Study and analysis of the effects of SiGe source and pocket-doped channel on sensing performance of dielectrically modulated tunnel FET-based biosensors. *IEEE Transactions on Electron Devices*, *63*(6), 2589-2596.
8. Ashok, T., & Pandey, C. K. (2023). Reduction of corner effect in ZG-ES-TFET for improved electrical performance and its reliability analysis in the presence of traps. *ECS Journal of Solid State Science and Technology*, *12*(7), 071005.
9. Pathakamuri, A. K., Pandey, C. K., & Ashok, T. (2024). Performance analysis of highly sensitive vertical tunnel FET for detecting light in near-IR range. *Journal of Materials Science: Materials in Electronics*, *35*(18), 1238.

10. Raad, B. R., Tirkey, S., Sharma, D., &Kondekar, P. (2017). A new design approach of dopingless tunnel FET for enhancement of device characteristics. *IEEE Transactions on Electron Devices*, *64*(4), 1830-1836.
11. Lay-Ekuakille, A., Koyazo, J. T., Chiffi, C., Singh, S. P., Rahman, M. Z. U., Rao, K. S., & Sravani, K. G. (2024). Measurements Under Biomechanical Stress in Medical Robotics: Diagnosing Pulmonary Impairments by Sensing Breathe Sounds. *IEEE Transactions on Instrumentation and Measurement*.
12. Guo, P. et al. "Tunneling field-effect transistor with Ge/$In_{0.53}Ga_{0.47}As$ heterostructure as tunneling junction." *Journal of Applied Physics* 113, 094502 (2013).
13. Pathakamuri, A. K., & Pandey, C. K. (2023). Impact of back gate-drain overlap on DC and analog/HF performance of a ferroelectric negative capacitance double gate TFET. Physica Scripta, 98(12), 124001.
14. Yadav, D. S., Verma, A., Sharma, D., & Sharma, N. (2018). Study of metal strip insertion and its optimization in doping less TFET. *Superlattices and Microstructures*, *122*, 577-586.
15. Pathakamuri, A. K., & Pandey, C. K. (2024). Performance investigation of ferroelectric L-shaped tunnel FET with suppressed corner tunneling for low power applications. *AEU-International Journal of Electronics and Communications*, *179*, 155314.
16. Jaya, M., & Lorenzo, R. (2024). Comprehensive review on charge plasma based junction less TFET biosensor. *Microsystem Technologies*, 1-21.
17. Pathakamuri, A. K., & Pandey, C. K. (2022, November). A novel extended back-gate negative capacitance TFET for improved device performance. In 2022 IEEE International Conference of Electron Devices Society Kolkata Chapter (EDKCON) (pp. 460-464). IEEE.
18. Kondaveeti, G. S., Kumar, R. A., & Karumuri, S. R. (2024). Design and Performance Analysis of N+ Pocket-Doped Vertical DMDGDP TFET with T-Shape channel for Sensitivity Improvement---As a Biosensor. *IEEE Sensors Journal*.
19. Kumar, A., & Kale, S. (2024). A comparative analysis of cavity positions in charge plasma based tunnel FET for biosensor application. *IETE Journal of Research*, *70*(3), 2819-2832.
20. Paul, R. (2023). Simulation and performance evaluation of charge plasma based dual pocket biosensor using SiGe-heterojunction TFET design. *Silicon*, *15*(5), 2147-2162.
21. Kumari, M., Singh, N. K., Kantipudi, V., & Sahoo, M. (2025). Design and investigation of charge plasma-based TMD heterojunction TFET biosensor for ultrasensitive detection. *Scientific Reports*, *15*(1), 15195.
22. Guo, P., Yang, Y., Cheng, Y., Han, G., Pan, J., Ivana, I., ... & Yeo, Y. C. (2013). Tunneling field-effect transistor with Ge/In0. 53Ga0. 47As heterostructure as tunneling junction. *Journal of Applied Physics*, *113*(9).
23. Synopsys, Sentaurus Device User Guide. Mountain View. CA. 2011
24. Smets, Q., Verhulst, A. S., El Kazzi, S., Gundlach, D., Richter, C. A., Mocuta, A., ... & Heyns, M. M. (2016). Calibration of the effective tunneling bandgap in GaAsSb/InGaAs for improved TFET performance prediction. *IEEE transactions on electron devices*, *63*(11), 4248-4254.
25. Sajjad, R. N., Chern, W., Hoyt, J. L., & Antoniadis, D. A. (2016). Trap assisted tunneling and its effect on subthreshold swing of tunnel FETs. *IEEE Transactions on Electron Devices*, *63*(11), 4380-4387.
26. Shreya, S., Khan, A. H., Kumar, N., Amin, S. I., & Anand, S. (2019). Core-shell junctionless nanotube tunnel field effect transistor: Design and sensitivity analysis for biosensing application. *IEEE Sensors Journal*, *20*(2), 672-679.
27. Anvarifard, M. K., Ramezani, Z., & Amiri, I. S. (2020). High ability of a reliable novel TFET-based device in detection of biomolecule specifies—A comprehensive analysis on sensing performance. *IEEE Sensors Journal*, *21*(5), 6880-6887.
28. Narang, R., Saxena, M., & Gupta, M. (2015). Comparative analysis of dielectric-modulated FET and TFET-based biosensor. *IEEE Transactions on Nanotechnology*, *14*(3), 427-435.

29. Choudhury, S., Baishnab, K. L., Guha, K., Jakšić, Z., Jakšić, O., & Iannacci, J. (2023). Modeling and simulation of a TFET-based label-free biosensor with enhanced sensitivity. Chemosensors, 11(5), 312.
30. Im, H., Huang, X. J., Gu, B., & Choi, Y. K. (2007). A dielectric-modulated field-effect transistor for biosensing. *Nature nanotechnology*, *2*(7), 430-434.
31. Chowdhury, N., Azad, S. F., &Khosru, Q. D. (2014). Negative capacitance tunnel field effect transistor: A novel device with low subthreshold swing and high on current. *ECS Transactions*, *58*(16), 1.
32. Das, A., Rewari, S., Kanaujia, B. K., & Gupta, R. S. (2022). Recent technological advancement in surrounding gate MOSFET for biosensing applications-a synoptic study. *Silicon*, *14*(10), 5133-5143.
33. Reddy, I. V. V., & Tripathi, S. L. (2021). Enhanced performance double-gate junction-less tunnel field effect transistor for bio-sensing application. *Solid State Electronics Letters*, *3*, 19-26.
34. Pathakamuri, A. K., Pandey, C. K., & Ghosh, P. (2024). Negative capacitance split source tunnel FET as dielectric modulated highly sensitive biosensor. *Microsystem Technologies*, 1-12.
35. Chong, C., Liu, H., Wang, S., Chen, S., & Xie, H. (2020). Sensitivity analysis of biosensors based on a dielectric-modulated l-shaped gate field-effect transistor. *Micromachines*, *12*(1), 19.
36. Dash, S., Mohanty, S. K., & Mishra, G. P. (2021). Segmented drain engineered tunnel field effect transistor for suppression of Ambipolarity. Silicon.
37. I. Chahardah Cherik and S. Mohammadi, "Vertical Tunneling Field-Effect Transistor With Germanium Source and T-Shaped Silicon Channel for Switching and Biosensing Applications: A Simulation Study," in *IEEE Transactions on Electron Devices*, vol. 69, no. 9, pp. 5170-5176, Sept. 2022, doi: 10.1109/TED.2022.3189326.